# Investigating the Neural Correlates of Pathological Cortical Networks in Alzheimer's Disease Using Heterogeneous Neuronal Models

Kamal Abuhassan*, Damien Coyle, *Member, IEEE*, and Liam P. Maguire

*Abstract*—This paper describes an investigation into the pathophysiological causes of abnormal cortical oscillations in Alzheimer's disease (AD) using two heterogeneous neuronal network models. The effect of excitatory circuit disruption on the beta band power (13–30 Hz) using a conductance-based network model of 200 neurons is assessed. Then, the neural correlates of abnormal cortical oscillations in different frequency bands based on a larger network model of 1000 neurons consisting of different types of cortical neurons are also analyzed. EEG studies in AD patients have shown that beta band power (13–30 Hz) decreased in the early stages of the disease with a parallel increase in theta band power (4–7 Hz). This abnormal change progresses with the later stages of the disease but with decreased power spectra in other fast frequency bands plus an increase in delta band power (1–3 Hz). Our results show that, despite the heterogeneity of the network models, the beta band power is significantly affected by excitatory neural and synaptic loss. Second, the results of modeling a functional impairment in the excitatory circuit shows that beta band power exhibits the most decrease compared with other bands. Previous biological experiments on different types of cultural excitatory neurons show that cortical neuronal death is mediated by dysfunctional ionic behavior that might specifically contribute to the pathogenesis of $\beta$-amyloid-peptide-induced neuronal death in AD. Our study also shows that beta band power was the first affected component when the modeled excitatory circuit begins to lose neurons and synapses.

*Index Terms*—Alzheimer's disease (AD), computational models, EEG, functional deficits, structural impairment.

## I. Introduction

**A**LZHEIMER'S disease (AD) is the most common neurodegenerative disorder associated with progressive dementia. The clinical symptoms of AD are cognitive and intellectual deficits, and behavior dysfunction. In most instances, symptoms develop gradually or precipitously. AD constitutes approximately 70% of all dementia cases and is expected to affect 1 in 85 people worldwide by 2050 [1]. It has a signifi-

cant impact on patients and caregivers, and generates substantial costs on health care providers in developed countries [2]. Clearly understanding the dynamics of neuronal networks in healthy and dysfunctional cortices is important and could aid in the development of effective diagnostic tools and prevention measures.

For the last few decades, EEG has been utilized for diagnosing dementias. EEG is a measure of the electrical activity along the scalp produced by a sufficiently large population of neurons. There is a strong correlation between cognitive deficit and the degree of the EEG abnormality. EEG spectral analysis in AD patients has shown a decrease in the mean frequency, alpha (8–12 Hz) and beta (13–30 Hz) band powers with a parallel increase in delta (1–3 Hz) and theta (4–7 Hz) band powers compared with those of healthy elderly subjects [3]. The attenuation of alpha band power is associated with an increase in lower alpha (8–10 Hz) band power and a parallel decrease in upper alpha (10–12 Hz) band power [4].

The EEG abnormalities in AD indicate functional and anatomical impairment of the cerebral cortex affected by the disease. More investigations are needed to provide insights to the underlying neurological basis of those abnormalities as well as to couple those findings with the severity of the disease. This study is targeted at investigating the relationship between AD EEG abnormalities and some neuropathological changes during AD using a conductance-based local neuronal network oscillating in beta band [5] and a simple larger network model of different types of cortical neurons that oscillates in different frequency bands [6].

The neuropathology of AD is characterized by an enormous neuronal and synaptic loss in the cerebral cortex and certain subcortical regions, and the formation of both neurofibrillary tangles (NFT) and neurotic plaques (NP) [7]. NFT are pathological tangles of hyperphosphorylated tau protein accumulated in the brains of AD patients; it is believed that the number of NFT is directly correlated with neuronal dysfunction as well as indicating the degree of dementia [8]. $\beta$-amyloid peptide (A$\beta$) is the main component of NP observed in the brains of patients with AD and has been suggested to contribute to the pathogenesis of neuronal degeneration [9].

A number of studies reported a deregulation of neuronal K+ channel function after exposure to A$\beta$ peptide fragments, which led to remarkable perturbations in neuronal behavior [10]–[12]. These channels provide a negative feedback to the membrane potential of neurons. Thus, it regulates the neuronal dynamics including the timing of interspike intervals (time between

spikes), setting the resting potential, and keeping action potentials short [13]. Therapeutic suggestions can be derived from computational models of dysfunctional neural behavior to slow down neural degeneration in AD.

The goal of this study is to elaborate and extend the findings in [14] and [15]. A recent modeling study of the hippocampal CA1 and medial septal regions has proposed that hippocampal theta band power is increased as a result of A$\beta$-induced reduction in A-type potassium current $I_A$ in *e*-cells [16]. This suggests the differential vulnerability of neurons and synapses in different cortical and subcortical areas to A$\beta$ fragments.

In this study, we examine the effects of neuronal/synaptic loss and deregulation of negative feedback to the membrane potential of cortical neurons (which mainly results from A$\beta$-induced dysfunctional K+ channels) on the oscillatory activity of cortical networks.

Firstly, the effect of excitatory circuit disruption on beta band power (13–30 Hz) is investigated using a local network model. Then, the investigation is extended to explore the underlying neurological sources of abnormal dynamics in different frequency bands based on a larger network model consisting of different types of cortical neurons.

The paper is outlined as follows. The network models are described in Section II. The results and analysis are provided in Section III. Finally, discussions and conclusion are presented in Sections IV and V, respectively.

## II. Network Models

### A. Local Neuronal Network

We simulated a conductance-based neuronal network of 200 cells containing 160 excitatory (*e*-cells) and 40 inhibitory (*i*-cells) neurons in the baseline (normal) case. The ratio of *e*- to *i*-cells is 4 (80%) to 1 (20%) motivated by the anatomy of the mammalian cortex [17]. The cells are connected all-to-all assuming that (*e–e*) synapses are weak within local networks [18]. Parameters and functional forms of the equations are adopted from [5].

Neurons were modeled by Hodgkin–Huxley dynamics; *i*-cells were of the form

$$C\left(\frac{dV_i}{dt}\right) = -g_L(V_i - V_L) - g_K n^4(V_1 - V_K)$$
$$- g_{Na}m^3h(V_i - V_{Na}) - I_{syn,i} + I_0 \quad (1)$$

and the *e*-cells were modeled by the equations

$$C\left(\frac{dV_e}{dt}\right) = -g_L(V_e - V_L) - g_K n^4(V_e - V_K)$$
$$- g_{Na}m^3h(V_e - V_{Na}) - g_{AHP}w(V_e - V_K)$$
$$- I_{syn,e} + I_0. \quad (2)$$

Both types of cells have a leak (*L*), transient sodium (Na), and delayed rectifier potassium (K) current. The *e*-cells have an additional after-depolarizing potential (AHP) resulting in a slow outward potassium current.

The maximal conductances were $g_{Na} = 100\,\text{mS/cm}^2$, $g_K = 80\,\text{mS/cm}^2$, $g_L = 0.1\,\text{mS/cm}^2$, and $g_{AHP} = 0.3\,\text{mS/cm}^2$. Reversal potentials were $V_L = -67$ mV, $V_K = -100$ mV, and $V_{Na} = 50$ mV. The capacitances for *e*- and *i*-cells were $1\,\text{AF/cm}^2$. Parameters for both the *e*- and *i*-cells were the same; the only differences are in the synaptic currents and the driving currents, $I_0$. The gating variables *m*, *h*, *n* satisfy equations of the form

$$\frac{dx}{dt} = a_x(V)(1 - x) - b_x(V)(x). \quad (3)$$

For *x = m, h, n* where

$$a_m(V) = \frac{0.32(54 + V)}{(1 - \exp([-(V + 54)/4]))} \quad (4)$$

$$b_m(V) = \frac{0.28(V + 27)}{(\exp([(V + 27)/5]) - 1)} \quad (5)$$

$$a_h(V) = 0.128 \exp\left[\frac{-(V + 50)}{18}\right] \quad (6)$$

$$b_h(V) = \frac{4}{(1 + \exp([-(V + 27)/5]))} \quad (7)$$

$$a_n(V) = \frac{0.032(V + 52)}{(1 - \exp([-(V + 52)/5]))} \quad (8)$$

$$b_n(V) = 0.5 \exp\left[\frac{-(57 + V)}{40}\right). \quad (9)$$

The gating variable *w* is represented by

$$\frac{dw}{dt} = \frac{(w_\infty(V) - w)}{\tau_w(V)} \quad (10)$$

$$w_\infty(V) = \frac{1}{(1 + \exp([-(V + 35)/10]))} \quad (11)$$

$$\tau_w(V) = \frac{400}{(3.3 \exp([(V+35)/20]) + \exp([-(V + 35)/20]))}. \quad (12)$$

Synaptic currents were modeled as follows:

$$I_{syn,\alpha} = g_{i\alpha}s_{i,\text{tot}}(V_\alpha - V_{in}) + g_{e\alpha}s_{e,\text{tot}}(V_\alpha - V_{ex}) \quad (13)$$

for $\alpha = \{e, i\}$.

Reversal potentials for AMPA and GABA$_A$ were $V_{ex} = 0$ mV and $V_{in} = -80$ mV, respectively. The synaptic gates satisfy:

$$s_{\alpha,\text{tot}} = \frac{1}{N_\alpha} \sum_{\alpha-\text{cells}} s_\infty \quad (14)$$

$$\frac{ds_\alpha}{dt} = a_\alpha\left(1 + \tanh\left(\frac{V_\alpha}{4}\right)\right)(1 - s_\alpha) - \left(\frac{s_\alpha}{\tau_\alpha}\right) \quad (15)$$

where $a_e = 20$/ms, $a_i = 1$/ms, $\tau_e = 2.4$ ms, and $\tau_i = 12$ ms. The inhibitory GABA$_A$ conductances, $g_{ie}$ and $g_{ii}$ are 5 mS/cm$^2$ and 10 mS/cm$^2$, respectively.

The excitatory conductances were $g_{ee} = 0.01$ mS/cm$^2$ and $g_{ei} = 0.05$ mS/cm$^2$. The model time was 2000 ms and spike trains were assessed after 1000 ms allowing a settlement period of 1000 ms. Gaussian noise generated by a wiener process was

added to the voltages at each integration step. The magnitude of the noise was 0.5 mV$^2$/ms for the e-cells. The equations were integrated using Euler's method with a time step of 0.025 ms.

To achieve heterogeneity, the input currents ($I_0$) were varied in the range from 0.6 to 2.0 $\mu$A/cm$^2$ to the e-cells and from 1 to 1.1 $\mu$A/cm$^2$ to the i-cells. The release of neuromodulators such as Acetylcholine (ACh) in the rest state is lower than that in the active states. Low ACh increases the AHP currents ($I_{AHP}$). This motivates the choice of relatively strong AHP currents ($I_{AHP}$) [5].

*1) Hypothesis Testing:* Based on the local network model, we have investigated the effect of excitatory circuit disruption on the beta band (13–30 Hz) power. To achieve our aim, we have first run the model with physiological (normal) values of all parameters for 25 trials. Then, we repeated the same procedure, but with the loss rate of e-cells varied in the interval (6–19)%, i.e., the number of e-cells ($N_e$) varied in the interval (130–150).

The fast Fourier transform (FFT) technique has been applied on the spiking train produced by each network setup to calculate the power spectra within the beta frequency band (13–30 Hz). One-way repeated measures ANOVA has been used to analyze the significance of the difference in beta band power between the physiological (baseline) case and cases with an abnormal ratio of e- to i-cells (corresponding to the AD groups). *P* values less than 0.05 indicate a significant difference.

## B. Larger Network Model

Spiking dynamics of neurons were simulated based on Izhikevich's model of spiking neurons [6], which can reproduce the firing patterns of all known types of hippocampal, cortical, and thalamic neurons. The spiking neuron can be expressed in the form of ordinary differential (16)–(18):

$$\frac{dV}{dt} = 0.04V^2 + 5V + 140 - u + I \qquad (16)$$

$$\frac{du}{dt} = a(bV - u) \qquad (17)$$

with the auxiliary after-spike resetting

$$\text{If } V \geq 30\,\text{mV, then } V \leftarrow c, u \leftarrow u + d \qquad (18)$$

where the dimensionless variables $V$ and $u$ represent the membrane potential and the recovery variable of the neuron, respectively. The recovery variable $u$ provides negative feedback to $V$, and it corresponds to the inactivation of Na+ ionic currents and activation of K+ ionic currents [6]. Dimensionless parameters $a$, $b$, $c$, and $d$ (illustrated in Fig. 1) can be tuned to simulate the dynamics of inhibitory and excitatory neurons. Parameter $b$ describes the sensitivity of the recovery variable $u$ to the subthreshold fluctuations of the membrane potential $V$. Greater values of $b$ couple $V$ and $u$ more strongly resulting in possible subthreshold oscillations and low-threshold spiking dynamics [6].

Spiking networks of 1000 neurons of different types, fully and randomly connected to each other with no plasticity, were simulated to investigate a number of hypotheses about the underlying causes of abnormal cortical oscillations in AD patients.
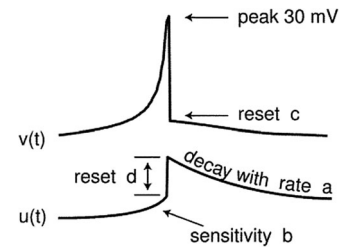


Fig. 1.    Graphical representation of the influence of parameters *a*, *b*, *c*, and *d* on the spiking dynamics. (Electronic version of the figure and reproduction permissions are freely available at www.izhikevich.com.)

TABLE I
CASE STUDIES

| Case study | Number of e-cells | Number of i-cells | Loss rate (%) of e-cells | Parameter b for e-cells |
|---|---|---|---|---|
| 1 | 764 - 794 [a] | 200 | 0.75% - 4.5% | 0.2 |
| 2 | 800 | 200 | 0 | 0.195-0.1995 [b] |

Model's setup for the investigated case studies. A number of parameters have been scaled to track the effect of changing such parameters on the EEG dynamics of the neuronal network.
[a]The loss rate of e-cells in case study 1 varies from 0.75% for group 1 to 4.5% for the last group. The length of step between each group in case study 1 is 0.25, i.e., the second group has 1% loss of e-cells. The total number of groups in case study 1 is 17 ([(794 − 764)/2] +1+ control group).
[b]Values of parameter *b* (17) for e-cells were decreased from 0.1995 (group 1) to 0.195 (group 10). The length of step between each group in case study 2 is 0.0005. The normal value of *b* for e-cells is 0.2.

The networks were stimulated by a random thalamic current at each time step. We have used MATLAB to simulate the networks in real time (resolution 1 ms). Setting the parameters of the model to physiological (normal) settings represents the physiological case. The ratio of excitatory to inhibitory neurons is 4 to 1 inspired by the anatomy of the mammalian cortex [6]. Model time was 30000 ms; spike trains were analyzed after 29000 ms allowing a settlement period (stability) of 29 s.

*1) Hypothesis Testing:* The model parameters are varied to test two hypotheses. The different group comparisons and associated parameter alterations have been categorized into the two case studies described in Table I. The first hypothesis is related to variations in the ratio of excitatory to inhibitory neurons in AD, while the second hypothesis is derived from AD observations of functional deficits in K+ ionic channels in cortical neurons. Each hypothesis was investigated with a computational model, as presented in Table I; each model has a different setup so that we refer to these models as case studies, i.e., hypothesis 1 was investigated in case study 1 and hypothesis 2 was investigated in case study 2.

Hypothesis 1 relies on the loss of excitatory neurons that affects the ratio of excitatory to inhibitory neurons in the cortical network and decreases the excitatory current in the network as a possible cause of abnormal network oscillations.

Hypothesis 2 links unbalanced cortical activity to an unbalanced negative feedback to the membrane potential. Specifically, it might result from dysfunctional K+ channels in excitatory neurons during AD. Hypothesis 2 suggests that the enhancement of negative feedback in excitatory neurons can be involved in abnormal oscillatory activity. This results in high-threshold spiking dynamics and less spiking activity for excitatory neurons.

To determine the overall rhythmic activity of the model in its control (normal) context, 10 trials of the model are run, each
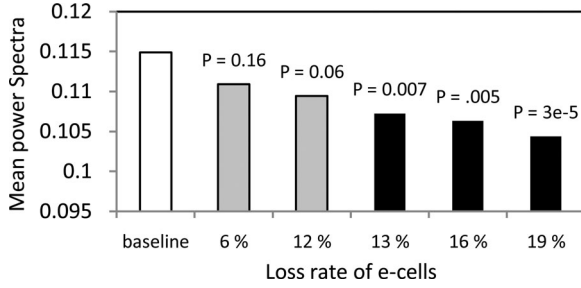
Fig. 2. Mean beta band power (13–30 Hz) for a physiological case (baseline) and cases with reduced *e*-cells. Differences (*P* values) measured by ANOVA are presented in the figure. Black bars correspond to significant differences. The number of trials is 25 for each setup.

TABLE II
MEAN POWER SPECTRA IN CASE STUDY 1

| Frequency band | Min. value | Control value | Decrease percentage |
|---|---|---|---|
| Delta | 3.498 | 3.737 | 6.4% |
| Theta | 2.71 | 3.104 | 12.7% |
| Alpha | 3.178 | 4.236 | 25% |
| Beta3 | 6.125 | 7.326 | 16.4% |
| Gamma | 13.15 | 15.034 | 12.5% |
| Full | 44.25 | 50.306 | 12% |

Minimum and control (physiological) values of the power spectra averages for slower and faster frequency bands in case study 1. Control value is the mean power spectra of the corresponding frequency band for the control group (10 trials) with physiological values of all model's parameters.

with random input, therefore, representing 10 individuals; the healthy control group. The model parameters are then modified to test each hypothesis. Again the model is run 10 times for each test, with each test representing a group with a certain neuropathology.

The FFT tool has been applied on the spiking train produced by each model to calculate the power spectra within the following frequency bands: delta (1–3 Hz), theta (4–7 Hz), alpha (8–12 Hz), beta1 (13–18 Hz), beta2 (19–21 Hz), beta3 (22–30 Hz), gamma (30–50 Hz), and full (1–70 Hz) bands; the categorization for the frequency bands is based on [19].

One-way repeated measures ANOVA has been used to analyze statistical significance of the difference in band power within each frequency band across the different groups, as outlined previously, *P* values smaller than 0.05 were considered statistically significant.

## III. RESULTS

### A. Decrease in Beta Band Power Induced by Loss of Excitatory Neurons and Synapses in the Local Network Model

A significant decrease in beta band power was observed after the excitatory circuit looses more than 20 *e*-cells (number of *e*-cells becomes ≤139, loss rate ≥13%, *P* < 0.05), as illustrated in Fig. 2.

We refer to this point as a breakdown point since the power spectra of beta rhythm exhibits a significant decrease after this point. In the network model, the death of each *e*-cell is associated with a synaptic loss of 319 excitatory synapses (1% loss of excitatory synapses) since the network is fully connected (each *e*-cell receives 159 e-synapses, innervates 159 *e*-cells, and has one recurrent synapse with itself).

The same response point appears after varying the network setup as follows: settlement period is increased to 2 s and power spectra differences are assessed based on the spike trains collected after second 2 until second 4. Thus, model time is 4 s.

### B. Effects of Varying the Number of Excitatory Neurons on the Oscillatory Activity of the Larger Network Model

In case study 1, the power spectrum averages of alpha and beta3 bands are significantly decreased when decreasing the number of *e*-cells ($N_e$) from 794 to 764 (loss% of *e*-cells is

increased from 0.75% to 4.5%). It is expected that reducing $N_e$ increases the amount of inhibition in the network and slows down the spiking activity, which explains the significant changes in the full band. From Table II, we can see that delta (slow rhythm) was not significantly affected, in contrast to the higher frequency bands.

Decrease percentage is calculated according to the following formula:

$$\text{Decrease}\% = \left( \frac{([\text{Control value}] - [\text{Minimum value}])}{[\text{Control value}]} \right) 100\%. \tag{19}$$

The minimum mean value was calculated by comparing the mean value of the power spectrum in the corresponding frequency band across all groups (each group contains 10 trials) in case study 1. We speculate that the power spectrum is shifted to lower frequencies with a parallel decrease in the coherence of fast rhythms, see Fig. 3(a). The statistical analyses show that the significant decrease started in beta3 band power ($N_e = 782$, 2.25% loss in *e*-cells).

This observation can be further explained by inspecting the minimum values of the power spectrum averages for slower and faster frequency bands, as given in Table II. The mean values of power spectrum for alpha and delta frequency band power for the groups in case study 1 are also presented in Fig. 3(b) and (c), respectively. The analyses show that the power spectrum in delta, theta, beta1, and beta2 bands was not significantly decreased.

### C. Effects of Varying Parameter b for e-Cells on the Oscillatory Activity of the Larger Network Model

The datasets in case study 2 contained important information about the magnitude of mean power ranges in high frequency bands. As presented in Table III, there are higher shifts from alpha, beta1, beta2, and beta3 band powers than slower frequency bands similar to previous observations for case study 1 outlined previously. The beta2 band is the most affected one. Again, decreasing parameter *b* (17) for *e*-cells upregulates the negative feedback *u* to the membrane potential *V* (16), which results in high-threshold spiking dynamics and decreases the spiking activity of *e*-cells. This accounts for the activation of $K^+$ ionic currents and inactivation of $Na^+$ ionic currents [6].

Values of parameter *b* (17) for *e*-cells were decreased from 0.1995 (group 1) to 0.195 (group 10). The length of decreasing
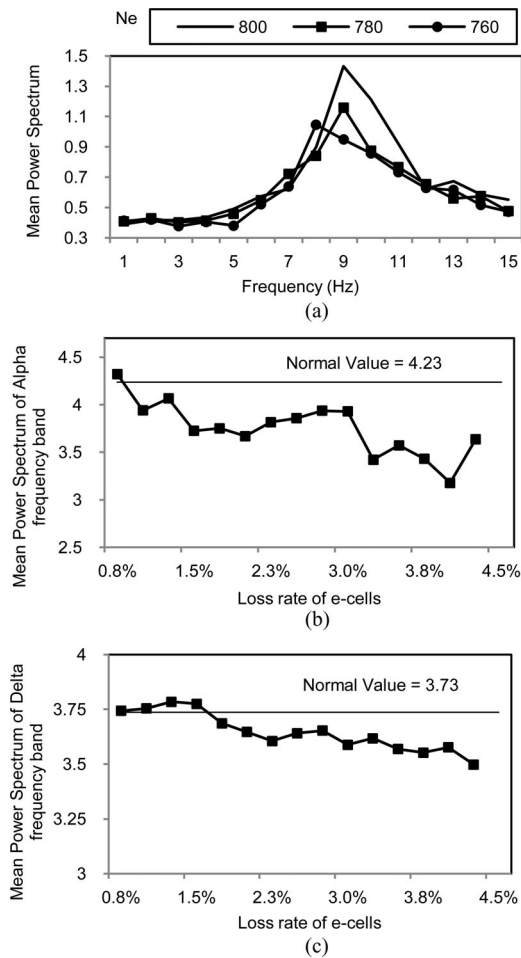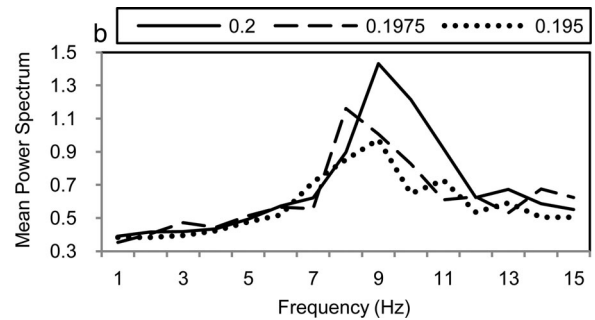
Fig. 3. Effects of increasing the loss rate of *e*-cells on the mean power spectrum. (a) Power spectrum is shifted to lower frequencies as more *e*-cells loss occurs. (b) and (c) Tracking the changes in alpha and delta band powers, respectively, as the number of *e*-cells is gradually decreased. The normal value (when $N_e = 800$ and the ratio of *e*- to *i*-cells is 4 to 1) of the mean power spectrum for delta and alpha frequency bands (control group) is indicated by a horizontal line.

TABLE III
MEAN POWER SPECTRA AFTER VARYING PARAMETER *b* FOR *e*-CELLS
(CASE STUDY 2)

| Frequency band | Min. value | Control value | Decrease percentage |
|---|---|---|---|
| Delta | 3.208 | 3.737 | 14.2% |
| Theta | 2.544 | 3.104 | 18% |
| Alpha | 2.937 | 4.236 | 30.7% |
| Beta1 | 2.671 | 3.579 | 25.4% |
| Beta2 | 1.105 | 1.787 | 38.7% |
| Beta3 | 5.359 | 7.326 | 26.9% |
| Gamma | 11.557 | 15.034 | 23.1% |
| Full | 39.326 | 50.306 | 21.8% |

Minimum and control (physiological) values of the power spectra averages for slower and faster frequency bands in case study 2.



Fig. 4. Effect of decreasing parameter *b* for *e*-cells on the mean power spectrum.

step for *b* (17) between the groups in case study 2 is 0.0005, i.e., value of parameter *b* for the second group is 0.199. Control (normal) value of parameter *b* (17) for *e*-cells is 0.2. The total number of groups in case study 2 is 11 ([(0.1995 − 0.195)/0.0005] + 1 + control group). The number of trials is 10 for each setup.

In Fig. 4, we demonstrate the simulated EEG signal for three groups with different values of parameter *b*.

## IV. DISCUSSION

### A. Structural Changes

It is commonly thought that an increase in theta band activity appears in the early stages of AD with a parallel decrease in beta activity; delta activity increases later during the course of the disease [3]. However, the underlying neural causes of abnormal EEG dynamics in AD are still poorly understood.

This research is concerned with developing a better understanding of the pathophysiological causes of abnormal cortical oscillations in AD based on a computational modeling approach.

In the current study, the effect of excitatory neural and synaptic loss on beta band power has been evaluated with two network models (along with other rhythms using the larger network model). Despite the heterogeneity of the network models, we show that the power spectrum of beta rhythm is significantly affected by excitatory neural and synaptic loss. In case study 1 (the large network model), we find that the significant decrease begins in the beta3 band (upper beta) when $N_e$ was 782 (2.25% loss in *e*-cells).

The sequence of gradual changes in faster bands is compatible with EEG studies [3]. Although the mean power spectrum of the full band is significantly decreased, slow bands (delta and theta) are only slightly affected by the decrease and most of the signal power was shifted from fast bands toward slow bands.

The decreased activity in alpha, beta, and gamma waves is related to changes in excitatory circuit activity [20]. The study involved the analysis of a large EEG dataset using global field synchronization (GFS), a novel measure to quantify global EEG synchronization [20]. A high GFS index for a certain frequency band reflects increased functional connectivity between brain processes. The patient's results showed increased GFS values in the delta band, and decreased GFS values in alpha, beta, and gamma frequency bands, supporting the disconnection syndrome hypothesis [20] and [21].

Other AD studies have reported decreased synchronization of alpha band in the early stages of AD [22]. In a previous study [4], we utilized a classical computational model of alpha rhythm proposed by [23] to explore the relationship between synaptic activities in a thalamocortical circuitry and diminished
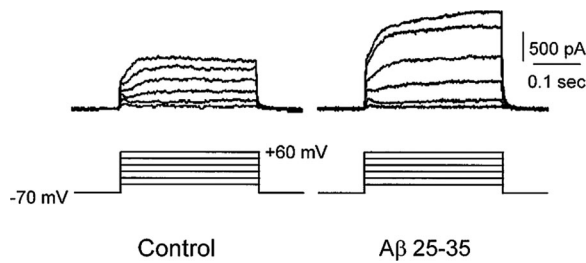
Fig. 5. Upregulation of $I_K$ by $\beta$-amyloid 25–35 in cortical *e*-cells [24]. (Reproduced with permission from S.P. Yu.)

## V. CONCLUSION

The impairment of excitatory circuitry appears to play an important role in abnormal oscillatory activity of the neuronal networks and this is supported by our study, which uses simple network models. Furthermore, the observation that the death of *e*-cells is preceded by dysfunctional behavior and changes in the ionic channels has been investigated in the study. The dynamical changes of the rhythmicity in the network as a result of alterations in the negative feedback for membrane potential in *e*-cells have been focused on. Future investigations will be based on a network consisting of 100 000 cortical neurons, distribution of axonal conduction delays, long-term spike-timing-dependent synaptic plasticity, receptor kinetics, and short-term plasticity. The network structure will be informed by the organization of the cerebral cortex [25].

alpha power. In [4], it was found that the deterioration in excitatory synaptic pathways during AD biased the dynamics toward increased inhibitory activity and affected alpha rhythmic activity.

In this study, we first traced the changes in alpha band power after the structural impairments in the excitatory circuit (case study 1). We observe similar changes in alpha band power, as proposed in [4]; see Fig. 3(a). Then, we further explored the consequences of functional deficits in excitatory circuits (case study 2) on alpha band power, see Fig. 4.

According to the simulation results, we speculate that the functional deficits of ionic channels contribute to abnormal alpha band power in AD.

### B. Functional Changes

It was demonstrated that cortical neuronal death is mediated by the enhancement of outward K+ current and such enhancement might specifically contribute to the pathogenesis of A$\beta$-induced neuronal death [24].

The results in [24] showed that A$\beta$ fragment 1–42 or 25–35 exposure induce an upregulation in the delayed rectifier K+ current $I_K$, an increase in maximal conductance, and a shift in its activation voltage relationship toward hyperpolarized levels, see Fig. 5.

Cortical neuronal cultures that contained cells from different layers of cortex were used in the experiments. The cells were excitatory because they responded to N-methyl D-aspartate (NMDA) or glutamate stimulation [24].

The upregulation of this type of K+ currents provides a more negative feedback to the membrane potential of *e*-cells followed by neuronal death. We speculate that the neural mechanism that underlies the sequence of abnormal changes into EEG of AD can be described by inspecting the results in case study 2, which showed a parallel significant decrease in different bands with a higher shift from upper frequency band powers, in particular, the power spectrum of beta2 and alpha rhythms. The significant decrease within beta band power appears also (before other rhythms) when decreasing $N_e$, followed by a breakdown in other frequency bands when $N_e$ decreases more and more (increased rate of neuronal and synaptic death).

## REFERENCES

[1] R. Brookmeyer, E. Johnson, K. Ziegler-Graham, and H. M. Arrighi, "Forecasting the global burden of Alzheimer's disease," *Alzheimer's Dementia*, vol. 3, pp. 186–191, 2007.

[2] C. W. Zhu and M. Sano, "Economic considerations in the management of Alzheimer's disease," *Clin. Interventions Aging*, vol. 1, pp. 143–154, 2006.

[3] J. Jeong, "EEG dynamics in patients with Alzheimer's disease," *Clin. Neurophysiol.*, vol. 115, pp. 1490–1505, 2004.

[4] B. Sen, D. Coyle, and L. Maguire, "A thalamo–cortico–thalamic neural mass model to study alpha rhythms in Alzheimer's disease," *Neural Netw. Special Issue Brain Disorders*, vol. 24, pp. 631–645, 2011.

[5] O. Jensen, P. Goel, N. Kopell, M. Pohja, R. Hari, and B. Ermentrout, "On the human sensorimotor-cortex beta rhythm: Sources and modeling," *NeuroImage*, vol. 26, pp. 347–355, 2005.

[6] E. M. Izhikevich, "Simple model of spiking neurons," *IEEE Trans. Neural Netw.*, vol. 14, no. 6, pp. 1569–1572, Nov. 2003.

[7] D. J. Selkoe, "Alzheimer's disease is a synaptic failure," *Science*, vol. 298, pp. 789–791, 2002.

[8] J. P. Brion, "Neurofibrillary tangles and Alzheimer's disease," *Eur. Neurol.*, vol. 40, pp. 130–140, 1998.

[9] J. A. Hardy and G. A. Higgins, "Alzheimer's disease: The amyloid cascade hypothesis," *Science*, vol. 256, pp. 184–185, 1992.

[10] A. Pannaccione, F. Boscia, A. Scorziello, A. Adornetto, P. Castaldo, R. Sirabella, M. Taglialatela, G. F. Di Renzo, and L. Annunziato, "Upregulation and increased activity of KV3.4 channels and their accessory subunit MinK-related peptide 2 induced by amyloid peptide are involved in apoptotic neuronal death," *Mol. Pharmacol.*, vol. 72, pp. 665–673, 2007.

[11] Y. Pan, X. Xu, X. Tong, and X. Wang, "Messenger RNA and protein expression analysis of voltage-gated potassium channels in the brain of Abeta(25-35)-treated rats," *J. Neurosci. Res.*, vol. 77, pp. 94–99, 2004.

[12] L. D. Plant, N. J. Webster, J. P. Boyle, M. Ramsden, D. B. Freir, C. Peers, and H. A. Pearson, "Amyloid beta peptide as a physiological modulator of neuronal 'A'-type K+ current," *Neurobiol. Aging*, vol. 27, pp. 1673–1683, 2006.

[13] S. G. Birnbaum, A. W. Varga, L.-L. Yuan, A. E. Anderson, J. D. Sweatt, and L. A. Schrader, "Structure and function of Kv4-family transient potassium channels," *Physio. Rev.*, vol. 84, pp. 803–833, 2004.

[14] K. Abuhassan, D. Coyle, and L. Maguire, "Simple spiking networks to investigate pathophysiological basis of abnormal cortical oscillations in Alzheimer's disease," *Irish J. Med. Sci.*, vol. 180, suppl. 2, pp. 62, 2011.

[15] K. Abuhassan, D. Coyle, and L. Maguire, "Employing neuronal networks to investigate the pathophysiological basis of abnormal cortical oscillations in Alzheimer's disease," in *Proc. 33rd Annu. IEEE Eng. Med. Biol. Soc. Conf.*, Boston, MA, 2011, pp. 2065–2068.

[16] X. Zou, D. Coyle, K. Wong-Lin, and L. Maguire, (2011, Jun.). Computational study of hippocampal-septal theta rhythm changes due to beta-amyloid-altered ionic channels, *PloS ONE* [Online], 6(6). Available: http://dx.plos.org/10.1371/journal.pone.0021579.

[17] V. Braitenberg and A. Schuz, *Anatomy of the Cortex: Statistics and Geometry*. Berlin, Germany: Springer Verlag, 1991.